Self-Consistent Reaction Field Calculations of Nonequilibrium Solvent Effects on Proton Transfer Processes through Low-Barrier Hydrogen Bonds

M. F. Ruiz-López,*,† A. Oliva,‡ I. Tuñón,§ and J. Bertrán‡

Laboratoire de Chimie Théorique, UMR CNRS-UHP 7565,|| Université Henri Poincaré, Nancy I, BP 239, 54506 Vandoeuvre-lès-Nancy Cedex, France, Unitat de Química Física, Universitat Autónoma de Barcelona, 08193 Bellaterra (Barcelona), Spain, and Departamento de Química Física, Universidad de Valencia, 46100 Burjasot, Spain

Received: August 5, 1998

We investigate dynamic solvent effects on proton transfer reactions in the strongly hydrogen-bonded hydroxyl−water model system by using a self-consistent nonequilibrium reaction field method. The initial motivation for the present work lies in the results of a recently reported molecular dynamics simulation for the same system in aqueous solution, carried out through combined density functional and molecular mechanics potentials. Such a study has confirmed that proton transfer occurs in an essentially frozen environment and that solvent fluctuations may play a crucial role in the reaction dynamics. Nevertheless, owing to the use of effective charge water models in molecular dynamics simulations, the effect of solvent electronic polarization, which can be assumed to respond instantaneously to solute charge modifications, cannot be accounted for explicitly. Our main goal in the present study is to analyze such an effect in the effective energy profile instantaneously experienced by the proton, using for this purpose ab initio methods and a dielectric continuum model of the solvent. Basically, the polarization of the solvent is divided into inertial and noninertial terms. The latter is assumed to be always in equilibrium with the solute whereas the former is characterized by a finite relaxation time. The model allows us to estimate the dependence of the activation energy and transition structure geometry on the solvent inertial polarization which is described by a fluctuating global solvent coordinate related to solute internal parameters. In some cases, the activation barrier may be lower than the equilibrium barrier. A detailed analysis of the effect of electronic polarization on the solute is also presented.

1. Introduction

Proton transfer (PT) occurs in many chemical and biochemical reactions, and therefore its study has wide interest.[1] Large environmental effects are expected for PT processes because, in general, they are accompanied by a substantial reorganization of the reactant charge distribution. For instance, the activation barrriers of a given reaction may be quite different in the gas phase and in polar solvents.[2] One of the most striking characteristics of PT reactions is that they usually take place on a very short time scale.[3] Hence, in a polar medium like water, the orientational relaxation time of solvent molecules may be substantially larger than the time for the reaction which in this case cannot be described in terms of equilibrium energy surfaces. Kurz and Kurz[4] proposed different mechanisms for proton transfer in solution representing extreme situations in which the solvent may be basically considered either as a thermal bath equilibrated with the solute along the reaction coordinate or as a fluctuating environment which may or may not assist the chemical process. According to this work,[4] when the activated complex has no equilibrium environment, the deviation of solvent configuration from its equilibrium state is expected to be toward that configuration which is appropriate for an internal structure in which the proton is half-transferred. This model is then related to the Marcus theory of proton transfer reactions.[5]

A few theoretical studies have been devoted to the nonequilibrium solvation effects on PT in hydrogen-bonded systems using continuum models.[6,7] In the work of Timoneda and Hynes,[6] the chemical system was simply described by a combination of diabatic valence bond states and the PT process in a model hydrogen-bonded complex was represented by changes of a point dipole. The authors studied the shape of free-energy surfaces for proton transfer between neutral molecules to produce an ion pair. Aguilar and Hidalgo[7] employed a parametrized model to study the influence of nonequilibrium solvation on free energy profiles for PT in $[H_3N\cdots H^+\cdots NH_3]$. Here, too, the solute was described by a simple polarizable dipole. In these works, the large dependence of the PT energy profile on solvent coordinate was demonstrated. This result confirmed the results obtained previously through the study of PT reactions in small clusters.[8]

Molecular dynamics (MD) simulations are, in principle, better adapted than continuum models to investigate dynamic solvent effects on reactions,[9] although computations are then limited by the approximate nature of the intramolecular interaction potential and reactant descriptions. Classical dynamics approaches using combined quantum mechanics (QM) and molecular mechanics (MM) potentials have been reported for PT processes in solution. The attention has been focused either on the calculation of free energy[10] or on the analysis of the influence of solvent dynamics on elementary reactive events.[11] Ab initio MD techniques have also been employed to study ion transport[12] and acid dissociation[13] in water. A quantum dynamical description of the nuclear degrees of freedom of the proton has been

† Université Henri Poincaré.
‡ Universitat Autónoma de Barcelona.
§ Universidad de Valencia.
|| Part of the Institut Nancéien de Chimie Moléculaire.

10.1021/jp983288b CCC: $15.00
Published on Web 12/05/1998

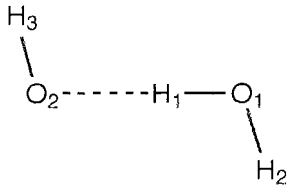

Figure 1. Schematic representation of the system studied. The system is planar and the O−H−O group is linear. The reaction coordinate **r** is defined as $\mathbf{r} = {}^1/_2$(O1H1 − O2H1).

considered through different MD implementations[14] demonstrating the crucial importance of quantum effects on the rate constants of many PT reactions.

Another interesting work was reported recently for the mechanism of HCl ionization in water.[15] This approach combines ab initio computations of potential energy surfaces of small clusters and statistical averaging via Monte Carlo simulations. The effect of solute polarization due to the solvent and that of solvent fluctuations on proton potential, as well as the quantum character of the proton nuclear motion, were examined in this paper in order to investigate the elementary steps of the ionization process.

In the present work, we revisit the theoretical analysis of nonequilibrium solvent effects on PT processes using an approach which complements the previous studies in this field. The idea is to exploit the possibilities offered by continuum models to treat accurately electronic polarization effects together with advanced MD simulation results obtained recently for the dynamic behavior of the solvent in PT reactions.[11] In the model used here,[16] the solvent is represented by a polarizable continuum medium and the solute is described by quantum mechanical methods. The solute−solvent interaction energy is computed by means of a full multipole development of the solute's charge distribution. The solvent response is characterized by inertial and noninertial polarization components. The former is assumed to be completely frozen during PT whereas the latter is always in equilibrium with the solute charge distribution. This model allows us to evaluate the PT potential energy surface for different values of the solvent polarization, which plays the role of a global solvent coordinate. We then discuss the effect of solvent fluctuations and nonequilibrium solvation on the instantaneous potential energy surface and the conditions under which the solvent may drive the reaction.

There are some aspects of the present work which may be related to previous studies investigating chemical reactions in strong electric fields.[17] In fact, the inertial solvent polarization may be regarded as a constant field (although not necessarily homogeneous) along the reaction path, provided the frozen-solvent hypothesis is made. It must be stressed, however, that in solution the noninertial polarization equilibrates the solute's charge distribution and therefore is far from being constant along the process.

As an example, we study the model system formed by a hydroxyl anion bonded to a water molecule in aqueous solution, which has been studied at different theoretical levels.[10−11,18−21] The system is schematically represented in Figure 1. PT from water to the hydroxyl anion is studied by assuming a planar trans structure, an OO distance of 2.5 Å, and a linear O−H−O arrangement, as represented in Figure 1 (note that high-level ab initio computations predict an equilibrium OO distance in the gas phase of 2.515 Å[19]). Equilibrium and nonequilibrium energy surfaces are computed. For each value of solute and solvent coordinates, we calculate the wave function of the solvated solute using a self-consistent reaction field (SCRF) approach that allows us to analyze the response of the chemical system to the fluctuating environment. Solute polarization is shown to play an important role in the reaction.

2. Solvent Model

We assume a dielectric continuum model for the solvent. The reactants are inside a cavity that has been created in this polarizable dielectric continuum. The solvent is polarized by the solute and creates an inhomogeneous electric field inside the cavity which polarizes in turn the solute charge distribution. Therefore, an iterative procedure must be carried out until self-consistent polarizations are reached. Let us first consider the solute−solvent equilibrium case.

At equilibrium, the electrostatic solvation energy may be written through a multipole moment development[22]

$$\Delta G_{\mathrm{solv}} = -\frac{1}{2}\sum_{L} R_L M_L \tag{1}$$

where

$$R_L = \sum_{L'} f^0_{LL'} M_{L'} \tag{2}$$

M_L ($L = l, m$) are the multipole moments of the solute's charge distribution, and $f^0_{LL'}$ are reaction field factors depending on the relative static dielectric permittivity of the medium ϵ_0 and on the cavity definition. A necessary condition for the reaction field factor not to be zero is that L and L' have the same parity. Details for the computation of the reaction field factors can be found in the original references.[22] In quantum mechanical computations, the Hartree−Fock expressions (or Kohn−Sham equations[23]) are modified to account for the solute−solvent interaction in such a way that the total energy, defined by the solute intrinsic energy plus the free energy of solvation, is minimized. This gives rise to a self-consistent reaction field (SCRF) approach. The multipole development converges in general quite rapidly, but contributions from the quadrupole ($l = 2$) or the octupole ($l = 3$) are often substantial and may be essential especially if the system is nonpolar. In our work, we shall limit the multipole development to $l = 3$ and use a simple ellipsoidal cavity shape.

The solvation energy must also include the cavitation, i.e., the energy required to create the cavity, and the dispersion energy. The cavitation energy may be evaluated in different ways[24] but is not of interest here since we assume that the cavity is invariant along the PT process. The dispersion energy is also expected to vary very little along the process and is not computed. Note that cavitation and dispersion energies have opposite signs and compensate for each other in part.

The reaction field evaluated through continuum models may be related to the time-averaged potential created by the solvent. However, in real solutions, the reaction field due to solvent molecules is not constant but fluctuates around its average value. To account for such fluctuations, the model described above has to be slightly modified. With this goal, the polarization of the solvent may be regarded as having inertial and noninertial polarization components.[6−7,16,25] The noninertial part is related to electron polarization of the solvent molecules and can be assumed to be always in equilibrium with the solute charge distribution, adapting instantaneously to any modification of that distribution. Conversely, the inertial part is related to orientational polarization and is characterized by a large relaxation time compared, for instance, to some vibrational movements

of the solute or to reaction time. Thus, the proton transfer in the system considered below is achieved in 20−30 fs (when the proton being transferred has the mass of deuterium) whereas the solvent relaxation time around the solute after a transfer process is on the order of 1 ps.[11] The inertial polarization is thus associated with the difference between the static, ϵ_0, and the optical (infinite frequency), ϵ_∞, dielectric constants.

In our work, nonequilibrium solute−solvent systems will be such that for a given solute geometry (1) the inertial solvent polarization term is fixed and different from the self-consistent (equilibrium) value corresponding to the current solute geometry, (2) the noninertial term is relaxed and is in equilibrium with the solute's charge distribution, and (3) the solute wave function is also relaxed so that it is in equilibrium with the solvent electric field (inertial + noninertial). The relaxation of the noninertial solvent polarization and solute's wave function must be achieved iteratively with a modified SCRF scheme that we outline below.

For any arbitrary solvent configuration, we write the reaction field as a sum of inertial and noninertial contributions:

$$R_L = R_L^{\text{inert}} + R_L^{\text{noninert}} \tag{3}$$

The last term is simply given by

$$R_L^{\text{noninert}} = \sum_{L'} f^{\infty}_{LL'} M_{L'} \tag{4}$$

where $M_{L'}$ holds for the solute charge distribution and $f^{\infty}_{LL'}$ is a reaction field factor for the infinite frequency relative dielectric permittivity, ϵ_∞. The inertial term may be written in a quite general way by using fictitious multipoles M_L^* corresponding to a hypothetical solute charge distribution that would generate such an inertial solvent polarization:

$$R_L^{\text{inert}} = \sum_{L'} (f^{0}_{LL'} - f^{\infty}_{LL'}) M_L^* \tag{5}$$

The corresponding solvation free energy is[16]

$$\Delta G_{\text{sol}} = -\frac{1}{2}\sum_{LL'} f^{0}_{LL'} M_{L'} M_L + \frac{1}{2}\sum_{LL'} (f^{0}_{LL'} - f^{\infty}_{LL'})(\Delta M_{L'})\Delta M_L \tag{6}$$

where $\Delta M_L = M_L - M_L^*$. The first term in the free energy expression is the equilibrium term, and the second term is always positive.

3. Computation Method

In this work, we have carried out ab initio computations at the RHF/6-31+G* level[26] using the Gaussian 92 program[27] modified to account for solvent effects with the SCRF method developed at Nancy.[22,28] Though this basis set is not expected to describe very accurately the properties of a hydrogen-bonded system, it is sufficient to analyze the main effects due to nonequilibrium solute−solvent interactions. A similar basis set (namely 6-31G**) was previously used in a similar study.[10] Diffuse functions on the oxygen atoms have been considered in our work to better describe the electronic charge distribution of the anion. Correlation energy has not been computed. The reason for this is that the solvation energy is correctly evaluated at the RHF level; i.e., the correlation energy is practically the same for the isolated and the solvated systems. This point has been discussed before in the case of proton transfer reactions.[29] Thus, adding the correlation term would modify the activation energies presented in this paper by a constant quantity but would not modify either the solute polarization response or the energetics changes due to solvent effects. The study of these properties is indeed our main objective here. Net atomic charges have been computed using the CHELPG method.[30]

The system HOH···OH$^-$ has been studied using a fixed distance OO (2.5 Å), a linear H··O··H arrangement, and trans planar structure. We must stress that our study is not intended to investigate hydroxyl migration in aqueous solution, which would require us to include a few discrete water molecules around the anion and compute the energy surface without geometric constraints. The reaction considered here is merely a model one in which the activation barrier is closely related to the OO distance. This model has been already employed in the literature.[10,11] For the same reasons, we do not perform a rigorous transition state location (or an intrinsic reaction coordinate computation), but we choose, as the schematic reaction coordinate, the coordinate **r**, which represents the position of the proton being transferred with respect to the middle OO distance, as defined in Figure 1. In gas phase, geometry optimization is carried out (except for the constraints noted above) for each value of the coordinate **r**. The obtained geometries are then used for solution computations without further geometry optimization. In solution, the energy profile is obtained by adding the electrostatic free energy of solvation of a given structure to the gas-phase potential energy. Including other contributions to the free energy along the reaction path (zero-point energy, thermal corrections to the enthalpy, entropic terms) is not trivial. But these contributions are expected to be little modified by the solvent so that they are not relevant for a qualitative discussion of solvent effects. Solution calculations have been carried out by assuming the following dielectric constants for water: $\epsilon_0 = 78.4$ and $\epsilon_\infty = 1.8$.

Finally, it must be noted that in the present work the solvent response is connected to its infinite and zero-frequency dielectric constants. A more detailed analysis would require us to treat the first (and maybe the second) solvation shell discretely. Though this can be done within the present continuum model (for instance, by assuming an electrostatically solvated supermolecule with fixed solvent coordinates), such a refinement would considerably complicate the discussion. For a deeper study, molecular dynamics simulations are certainly promising, and this can already be done using combined QM/MM models[11,31] or the empirical valence bond approach,[32] which has been widely employed to investigate dynamics of reactions in solution and enzymes.[33]

4. Results

Before presenting our results, let us comment on previous theoretical studies carried out for the HOH···OH$^-$ hydrogen-bonded system.

Ab initio computations[18−20] in the gas phase predict a double-well energy profile, although another calculation with a smaller basis set leads to a single-minimum profile for the HO···H··· OH symmetric structure.[10] In aqueous solution, the medium effect favors the localization of charge, i.e., the asymmetric HOH···OH$^-$ system. The activation barrier for the proton transfer has been also estimated using MP2/6-31+G* energy calculations at HF/6-31+G* optimized geometries both in the gas phase and in aqueous solvent.[18] In the gas phase, the barrier was predicted to be very small (0.37 kcal/mol). Using a continuum model for the solvent and the same computational level, the barrier was predicted to increase by about 3 kcal/mol, leading to an activation energy of 3.15 kcal/mol, very close to the value obtained with a supermolecule approach, 3.55 kcal/

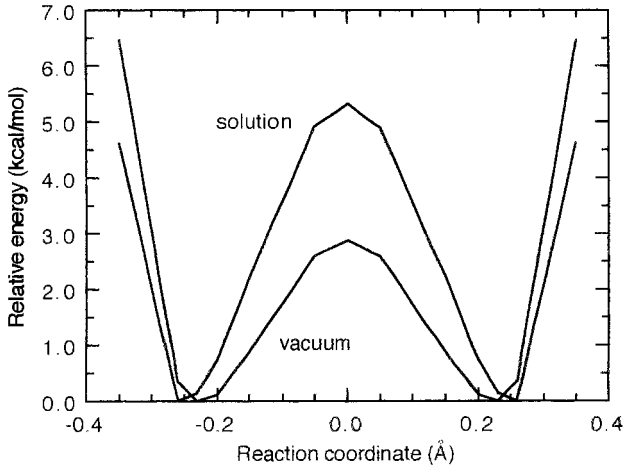

Figure 2. Energy profiles in the gas phase and in equilibrium aqueous solution.

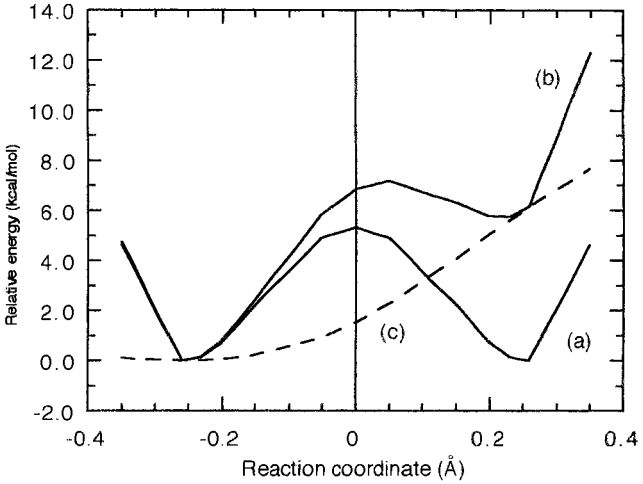

Figure 3. Energy profiles in equilibrium (a) and nonequilibrium (b) aqueous solution. The nonequilibrium case corresponds to a frozen solvent at the reactant inertial polarization. The dashed line (c) is the nonequilibrium solvation energy contribution to the total energy, so that (b) = (a) + (c).

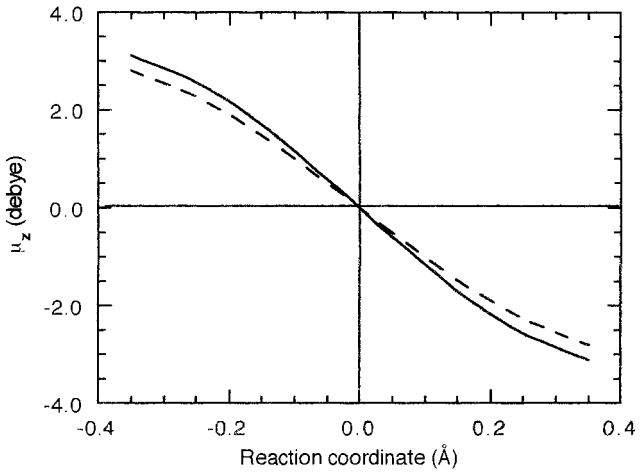

Figure 4. Variation of the dipole moment in the gas phase (dashed) and in equilibrium aqueous solution (solid line). The dipole moment was computed at the middle OO point. Only the component along the OO axis is shown.

mol,[18] and agreeing rather well with experimental estimations ranging from 2.1 to 4.8 kcal/mol.[34]

Recently, MD simulations[11] for HOH···OH^- in water solution were reported using a combined QM/MM approach: density functional theory and the TIP3P[35] potential have been used to describe the reactant HOH···OH^- and the solvent water molecules, respectively. After equilibration of the whole system, the final simulation was carried out during 6 ps using a time step of 0.2 fs (only the OO distance in the solute was constrained[36]). During this simulation time, a few reactive events were observed. The proton transfer requires about 20−30 fs and therefore proceeds in an essentially frozen environment. Indeed, the response of the solvent is delayed by about 50 fs. The solvent behavior was analyzed in terms of the electric field created by the TIP3P water molecules on the QM reactant at the middle point of the OO distance. It was shown that, in the equilibrated reactant distribution, this electric field may fluctuate by 50% with respect to its average value. In summary, the dynamics of the chemical system cannot be described through equilibrium conditions and solvent fluctuations may be expected to play a crucial role in the reaction. Note that, in these simulations, the hydrogen atom involved in proton transfer had the mass of deuterium.

We evaluate below the instantaneous potential energy surfaces for different frozen-solvent configurations in order to investigate the influence of the fluctuating environment. But for comparison purposes, we first compute the energy profiles in the gas phase and in solution, assuming solute−solvent equilibrium.

4.1. Energy Profile in the Gas Phase and in Solution at Equilibrium. The energy profiles in the gas phase and in aqueous solution at equilibrium are plotted in Figure 2. Since, in these computations, the OO distance is constrained, the curves in Figure 2 cannot be directly compared to the fully optimized geometry case.[18] However, the predicted solvent effect on the energy barrier for PT is quite comparable (an increase of about 3 kcal/mol). Note that the positions of the minima are slightly shifted in solution so that the water OH bond participating in the hydrogen bond is shorter. Hereafter, we call $\mathbf{r}_R^{sol}$ the value of $\mathbf{r}$ at the reactants in solution (roughly $\mathbf{r}_R^{sol} = -0.26$ Å, with O1H1 = 0.99 Å and O2H1 = 1.51 Å). Likewise, $\mathbf{r}_P^{sol}$ will represent the value of the reaction coordinate at the product in solution ($\mathbf{r}_P^{sol} = -\mathbf{r}_R^{sol}$). The electrostatic solvent effect clearly disfavors proton transfer when the equilibrium hypothesis is assumed.

4.2. Role of Inertial Solvent Polarization. The equilibrium curve in Figure 2 is not of much interest for the PT dynamics in solution since, as noted above, the proton transfer is a very fast process and the solvent cannot equilibrate the solute charge distribution along the reaction path. As a limit situation, we can reasonably assume that the PT process occurs in a frozen-solvent configuration. The simplest hypothesis consists of the assumption that the transfer proceeds in the solvent inertial reaction field which corresponds to the reactants in equilibrium, i.e., when the proton coordinate is $\mathbf{r} = \mathbf{r}_R^{sol}$. We call this case the "frozen solvent at the reactants". As shown in Figure 3, the corresponding energy profile displays a considerable higher energy barrier than the equilibrium curve since the nonequilibrium contribution (the second right-hand term in eq 6) increases as the chemical system goes to the TS and the products. The variation of such a term is also shown in Figure 3. It may be interesting to note that the main contribution to the nonequilibrium solvation contribution arises from the dipole moment $\mathbf{m}$, whose dependence on $\mathbf{r}$ is shown in Figure 4. If electron polarization is neglected, the dipole moment contribution to the nonequilibrium energy is simply given by

$$\Delta G_{l=1}^{non-eq} = \frac{1}{2}(f^0 - f^\infty)|\boldsymbol{\mu}(\mathbf{r}) - \boldsymbol{\mu}(\mathbf{r}_R^{sol})|^2 \qquad (7)$$

(for simplicity we write f^0 and f^∞ the reaction field factors for $L = 1$). This quantity represents the largest contribution to the nonequilibrium solvation energy drawn in Figure 3, but we show below that higher multipoles and nonadditive terms due to electronic polarization cannot be neglected.

This nonequilibrium solvation effect has other consequences too. Now, the position of the energy maximum ($\mathbf{r} = +0.05$ Å) does not correspond to the symmetric structure ($\mathbf{r} = 0.0$ Å) but is shifted toward the product and at the same time the position of the product is shifted toward smaller **r** values. Note also that the relative energy of the product with respect to the reactant is large and that the inverse process product → reactant in this reactant-like reaction field is quite easy. Indeed, due to the variation of the nonequilibrium solvation energy, the frozen-solvent curve for PT may present no minimum at the product side. An example was recently found for a model of the catalytic triad in serine proteases.[37]

The above results may be explained in terms of valence bond language by assuming two main solute configurations: HOH···OH^- and HO^- ···HOH which have symmetric diabatic curves (one could also take $HO^-\cdots H^+\cdots OH^-$ but it is not essential for a qualitative scheme). The frozen-solvent field is reactant-like so that it destabilizes the product diabatic curve (compared to equilibrium curve). Accordingly, activation energy increases and the TS is located at higher values of the reaction coordinate.

The previous frozen-solvent process is not a general case. In principle, PT may occur in any arbitrary frozen-solvent configuration reached by fluctuations. The probability of a given fluctuation can, in principle, be evaluated through the corresponding Boltzmann factors, but as mentioned above, one may expect the solvent fluctuations to modify the reaction field by about 50% in this system.[11] Accordingly, it is interesting to compute the shape of PT energy curves by considering a series of hypothetical frozen reaction fields with magnitudes falling within this range.

For this purpose, it is convenient to introduce the concept of a global solvent reaction coordinate. Following previous works,[16,25e,38] we define a generalized solvent coordinate in which an arbitrary inertial polarization field is expressed in terms of the equilibrium inertial polarization for other locations along the solute reaction coordinate. In this way, the generalized solvent coordinate **s** is connected with the solute reaction coordinate and may be defined as $\mathbf{s} = \mathbf{r}_s$, where $\mathbf{r}_s$ is the reaction coordinate having the appropriate equilibrium inertial polarization. Obviously, solvent fluctuations may be more general, but this approach allows us to simplify the discussion. One may also note that, for the dipolar solvation contribution, because the reactant dipole moment is basically directed along the OO axis, only the solvent electric field component along this axis is relevant. In this particular case, solvent coordinates can always be related to values of the reaction coordinate **r**.

Fluctuations of **s** around its average value at the reactants are then defined by $\mathbf{s} = \mathbf{r}_R^{sol}(1 - \delta)$. We must now choose values of δ for which the solvent electric field varies at most by 50% with respect to its average value. This roughly holds for $|\delta| \leq 0.5$ since, on one hand, we assume a linear response approximation and, on the other hand, the solute dipole moment varies approximately linearly with **r** (see Figure 4). The energy profiles for PT corresponding to various values of δ are displayed in Figure 5. As before, each curve in Figure 5 is obtained by adding to the equilibrium curve a nonequilibrium energy contribution (similar to that shown in Figure 3) which is zero at $\mathbf{r} = \mathbf{r}_R^{sol}(1 - \delta)$ and positive elsewhere.

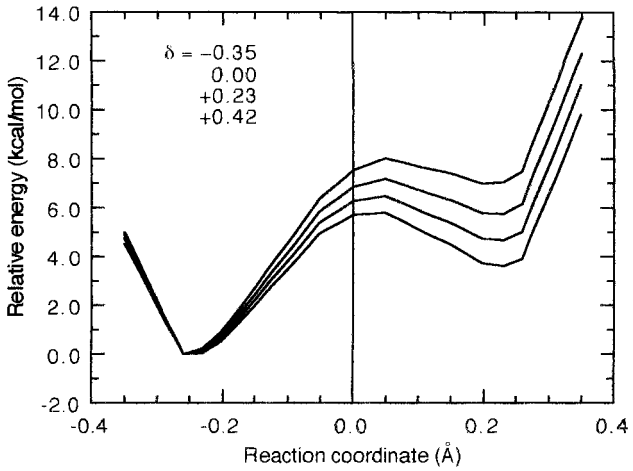

Figure 5. Energy profiles for proton transfer under different nonequilibrium conditions resulting from solvent fluctuations around the reactant configuration.

Two main cases must be considered in Figure 5. Solvent fluctuations toward the TS, i.e., those with $\delta > 0$, lead to a barrier decrease and product stabilization when compared to the energy profile for the frozen solvent at the reactants, i.e., for $\delta = 0$. Fluctuations with $\delta < 0$ lead to the opposite effect. In summary, fluctuations toward the TS assist the PT process although for the amplitudes considered (halfway between the reactant and TS) the barriers are still larger than the equilibrium barrier.

The previous conclusion requires two comments. First, the actual variation of the nonequilibrium term (second right-hand term of eq 6) strongly depends on the chemical system and determines in part the probability of solvent fluctuations. Second, large medium polarization perturbations may be achieved through mechanisms other than solvent fluctuations at equilibrium. For instance, electric field fluctuations in enzyme active sites may be generated by charged or polar groups in the protein[33] and may be a source of reaction activation.[39] In the case of reactions in solution with stepwise mechanisms, solvent relaxation between consecutive steps may be incomplete, giving rise to substantial nonequilibrium effects. The system considered here may be used to illustrate the latter case.

The combined DF/MM MD simulations carried out for HOH···OH^- in water solution[11] predicted that the time separating two consecutive reactive events (forward and backward proton transfer) is of the same order of magnitude as the solvent relaxation time, about 1 ps. Such a PT frequency is however an average value, and actually consecutive reactive events may occur a little faster or slower. In many cases, therefore, the process may proceed in an incompletely relaxed solvent, quite far from equilibrium conditions.

To account for such nonequilibrium effects, we consider now the PT energy surface for solvent coordinate $\mathbf{s} = \mathbf{r}_R^{sol}(1 - \delta)$ with $|\delta| \geq 0.5$. In particular, TS-like ($\delta \approx 1$, $\mathbf{s} \approx 0$) or product-like ($\delta \approx 2$, $\mathbf{s} \approx \mathbf{r}_P^{sol}$) solvent configurations are interesting. As before, the inertial polarization of the solvent is frozen along the reaction path. The energy profiles for different values of δ are shown in Figure 6 and are compared to the curve with $\delta = 0$ (frozen solvent at the reactant; see Figure 3). The PT energy barrier for either $\delta = 1$ (3.9 kcal/mol) or $\delta = 2$ (1.0 kcal/mol) is substantially smaller than that for $\delta = 0$ (7.2 kcal/mol) and even than the equilibrium barrier (5.3 kcal/mol; see Figure 2). Therefore, for TS-like and product-like **s** coordinates, the proton transfer becomes much easier. With respect to the $\delta = 0$ curve, the reactant energy minimum is shifted toward the TS whereas

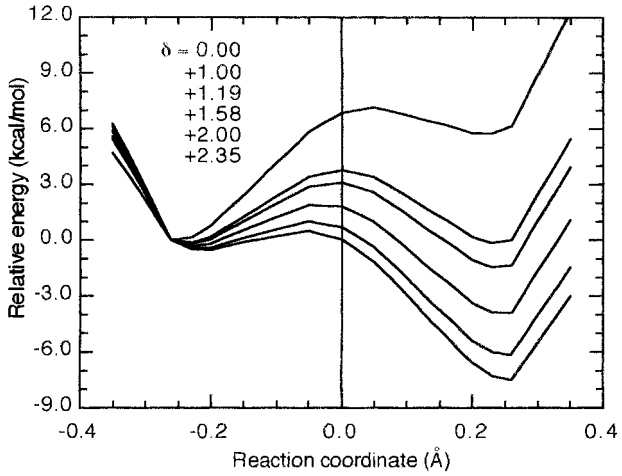

Figure 6. Energy under different nonequilibrium conditions arising from incomplete solvent relaxation (see text for explanation). For comparison, the frozen solvent at the reactant case ($\delta = 0$, top curve) is included.

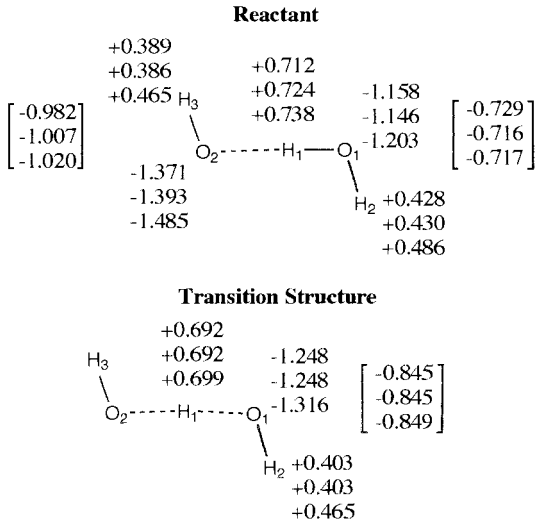

Figure 7. Net atomic charges for the reactant ($\mathbf{r} = -0.26$) and the transition structure ($\mathbf{r} = 0.0$). From top to bottom: gas phase, solution with only dipole moment contribution, solution with contributions up to $l = 3$. In brackets: total charges for OH groups.

the TS is shifted toward the reactants and the product minimum is shifted toward higher $\mathbf{r}$ values. Obviously, for $\delta = 1$ (TS-like solvent polarization), the curve is symmetric. Proton donation through a barrierless process may be expected for solvent coordinates slightly beyond the product value.

4.3. Role of Electronic Polarization. In Figure 7, we give the net atomic charges of the main structures, i.e., the reactant ($\mathbf{r} = \mathbf{r}_R^{sol}$) and transition structure ($\mathbf{r} = 0$), for the isolated and solvated species at equilibrium. In solution, two computations have been done limiting the maximum value of the multipole development to 1 or 3. In this way, the role of the dipolar term is emphasized. One sees that, in the reactant, the hydroxyl net charge becomes more negative through the effect of the solvent whereas the O1H2 group in the water molecule becomes less negative and the proton H1 becomes more positive. Hence, there is a net transfer of electron density from water to the hydroxyl group. One may note that the dipole moment contribution is large although higher multipoles enhance the charge transfer and tend to polarize the OH bonds. In the TS, the computation limited to $l = 1$ does not alter the charge distribution of the gas (as expected, since the structure has a center of symmetry)

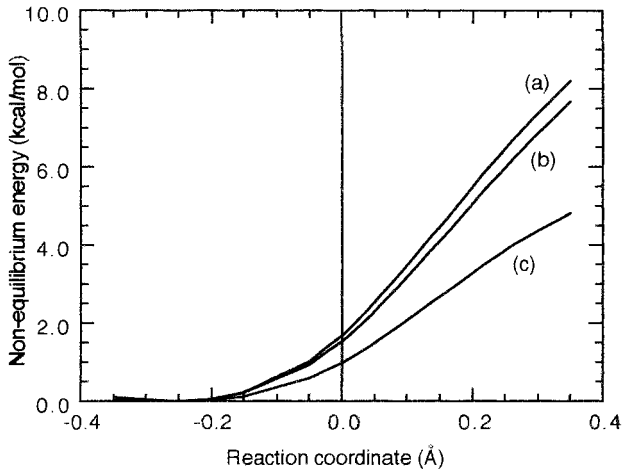

Figure 8. Nonequilibrium solvation energy contribution for $\mathbf{s} = \mathbf{r}_R^{sol}$: (a) multipole moments up to $l = 3$ are included, but the electronic polarization after solvent perturbation is not accounted for; (b) same as (a), but electronic polarization is included; (c) the calculation was limited to the dipole moment, $l = 1$, and the electronic polarization is included.

whereas the computation limited to $l = 3$ polarizes the two equivalent OH subunits and produces a slight charge transfer from the proton being transferred.

Let us now study the effect of electronic polarization on proton transfer when nonequilibrium solvation is considered. To simplify the discussion, we consider only the case $\mathbf{s} = \mathbf{r}_R^{sol}$. We want to evaluate the free energy difference between a solute−solvent system in equilibrium and out of equilibrium for given solute geometries in two cases: electronic solute relaxation after the perturbation is neglected or computed by solving the SCRF equations. In Figure 8, we plot this free energy difference for solute structures along the reaction path. The role of the solute electronic polarization (compare curves a and b) is not negligible and slightly counterbalances the destabilizing effect of the nonequilibrium reaction field. For comparison, we also give the values when the multipole expansion for the solute−solvent interaction is limited to the dipole moment. The contribution of higher multipoles cannot be neglected (compare curves b and c) since it is as large as that coming from the dipole moment alone.

The nonequilibrium solvation energy component (see eq 6) introduces a force acting on the solute's nuclei that, when $\mathbf{s} = \mathbf{r}_R^{sol}$, is responsible for the shift of the transition state position in the reaction path toward the products, as explained before. A more detailed analysis of the forces acting on the reaction coordinate is shown in Figure 9. When solute−solvent equilibrium is assumed, the total force is negative between the reactant and the transition state, positive between the TS and the product, and zero for these three stationary points. When nonequilibrium solvation is considered, an additional force term has to be added. Such a component for $\mathbf{s} = \mathbf{r}_R^{sol}$ is plotted in Figure 9 in the polarizable and nonpolarizable solute model cases. It is zero at the reactant (since the reactant is equilibrated with the solvent) but is negative beyond it, since the inertial solvent polarization creates a force on the chemical system which tends to recover the reactant structure. A maximum (in absolute value) is reached at about $\mathbf{r} = 0.15$ Å for both, the total force at equilibrium and the nonequilibrium component. When the solute is allowed to polarize, the magnitude of the restoring force decreases slightly; i.e., the relaxation of the solute electronic charge distribution tends to compensate in part the shift of the TS due to nonequilibrium solvation.

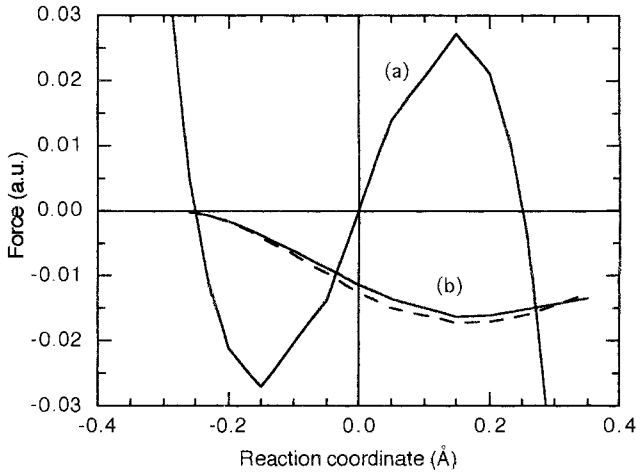

Figure 9. Forces acting on the reaction coordinate: (a) force at equilibrium; (b) additional force that appears after changing the equilibrium inertial solvent polarization to $\mathbf{s} = \mathbf{r}_R^{sol}$ (the dashed line does not include electronic polarization after solvent perturbation).

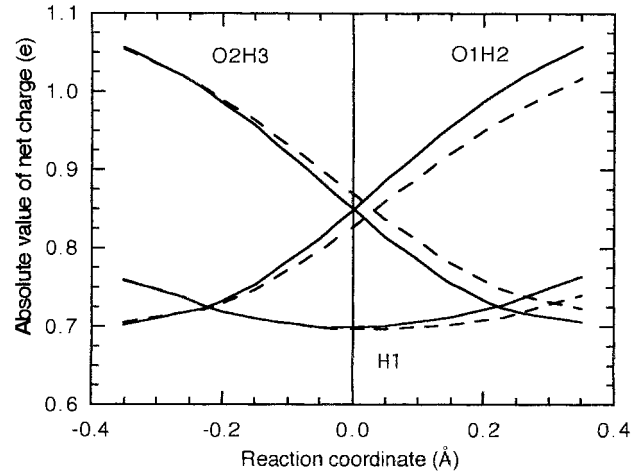

Figure 10. Variation of the absolute value of the net atomic charges (note that OH groups carry a negative charge) along the reaction coordinate. The solid lines correspond to the equilibrium case whereas the dashed lines correspond to the nonequilibrium case $\mathbf{s} = \mathbf{r}_R^{sol}$.

Some interesting features appear if one analyzes the variation of the net atomic charges along the reaction coordinate, which is shown in Figure 10 for equilibrium and nonequilibrium reaction paths. When equilibrium is assumed, the three curves are symmetric with respect to the TS position, $\mathbf{r} = 0$, where $q(\text{O1H2}) = q(\text{O2H3}) = -0.85$. One notes that, for a given value of the reaction coordinate between the reactant and the product, q(O2H3) is larger and q(O1H2) smaller (in absolute values) for the nonequilibrium process. The isoelectronic point $q(\text{O1H2}) = q(\text{O2H3})$ in the frozen-solvent process appears at $\mathbf{r} = +0.03$ Å, beyond the equilibrium TS position (note that the value of the net charge is roughly unchanged; i.e., $q(\text{O1H2}) = q(\text{O2H3}) = -0.85$). This result is easy to understand. As shown in Figure 7, the equilibrium solvent effect on the reactant favors electronic charge transfer from water to hydroxyl. In the frozen-solvent process, the inertial solvent polarization of a given structure along the reaction path must be replaced by the inertial polarization of the reactants ($\mathbf{s} = \mathbf{r}_R^{sol}$). The effect is an electronic polarization of the solute favoring the reactant charge distribution, which is opposed to the reaction advance from the electronic viewpoint. The definition of net atomic charges is not unambiguous, but it is clear that there is a relationship between the position of the TS and equalization of the net charge on the OH groups. Indeed, the energy maximum is at $\mathbf{r} = +0.05$ Å (see Figure 3), not far from the isoelectronic point ($\mathbf{r} = +0.03$ Å).

Although we do not describe in detail here other possible nonequilibrium situations, one can make a qualitative prediction based on the previous results. For instance, if the nonequilibrium solvation configuration is TS-like ($\mathbf{s} \approx 0$), one may expect the reaction field to modify the reactant electronic cloud so that the negative charge will be partially delocalized on the two OH groups, as happens for the TS. This means that it will assist the charge transfer and facilitate proton transfer. The same effect could be obtained by applying a constant electric field to the isolated reactant. This case has been discussed in detail before,[8] and it has been shown that appropriate fields may lead to large catalytic effects. For instance, in the case of an S_N2 process, the electric field was shown to polarize the reactant in such a way that the densities at critical points of the bonds being created and broken change toward the product.[8]

5. Conclusions

Because PT in low-barrier hydrogen bonds is a fast process, equilibrium solvation is not possible during such a reaction and the relevant energy profile must be obtained adopting a frozen-solvent hypothesis. By "frozen solvent" it must be understood that the inertial polarization component of the solvent is fixed to a definite value during PT. There is also a noninertial component which is related to electronic polarization of the solvent. The simplest approximation consists of the assumption that the solvent is frozen to its equilibrium value in the reactants. We have shown that, for the reaction studied, this introduces a more or less quadratic nonequilibrium solvation energy which destabilizes all the structures along the reaction coordinate with respect to the reactant. The transition structure appears later in the reaction coordinate and the activation energy is larger, compared to equilibrium results. The product energy minimum is also raised. Therefore, this nonequilibrium or dynamic solvent effect disfavors the transfer process.

However, solvent fluctuations must also be considered. In the present case, when fluctuations are such that they decrease the solvent polarization, the energy barrier is lowered. Previous MD simulations for this system have shown that fluctuations for which solvent polarization is intermediate between the reactant and the transition state are rather frequent. Then, the instantaneous barrier for PT may be comparable to the equilibrium case since the reactants and the TS are destabilized by a comparable amount. In the same simulations, it was also shown that the solvent relaxation time is large compared to the time separating consecutive proton transfer events in the chemical system, so that large nonequilibrium effects are expected. When PT arises in TS-like ($\mathbf{s} \approx 0$) or product-like ($\mathbf{s} \approx \mathbf{r}_P^{sol}$) solvent configurations, the energy barrier is smaller than the equilibrium barrier and the process becomes much easier.

Nonequilibrium effects influence the electronic charge distribution of the solute. Analysis of this distribution along the reaction path with $\mathbf{s} = \mathbf{r}_R^{sol}$ shows that electronic polarization of the solute tends to compensate the shift of the TS. In other words, the reaction is retarded by nonequilibrium effects both geometrically (the TS appears later) and electronically (the charge transfer among hydroxyl groups is delayed). This result illustrates the suitability of the SCRF model, in which an accurate computation of the polarized wave function is carried out at each step of the reaction coordinate.

Acknowledgment. M.F.R.-L. acknowledges financial support from the Spanish Ministerio de Educación y Ciencia for a 4 month stay at the Unitat de Química Física at Bellaterra and the members of this department for their warm hospitality. I.T. acknowledges a postdoctoral contract from the Spanish MEC and financial support from DGCYT Project No. PB96-0792. The authors are also grateful for financial support from the Picasso Program (Action Nos. 267B and 96121).

References and Notes

(1) Bell, R. P. *The Proton in Chemistry*, 2nd ed.; Chapman and Hall: London, 1973. Fersht, A. R. *Enzyme Structure and Mechanism*, 2nd ed.; W. H. Freeman & Co.: New York, 1985. *Electron and Proton Transfer in Chemistry and Biology*; Müller, A., Ratajczak, H., Junge W., Diemann, E., Eds.; Studies in Physical and Theoretical Chemistry, Vol. 78; Elsevier: Amsterdam, 1992. *Proton Transfer in Hydrogen-Bonded Systems*; Bountis. T., Ed.; Plenum: New York, 1993. Special issues on proton transfer: *Faraday Discuss. Chem. Soc.* **1982**, No. 74; *Chem. Phys.* **1989**, *136* (2); *J. Phys. Chem.* **1991**, *95* (25), 5.

(2) Reichardt, C. *Solvent Effects in Organic Chemistry*; Verlag Chemie: New York, 1979.

(3) Grunwald E.; Price E. *J. Am. Chem. Soc.* **1964**, *86*, 2970. Kreevoy, M. M.; Kretchmer, R. A. *J. Am. Chem. Soc.* **1964**, *86*, 2435. Kreevoy, M. M. *Adv. Phys. Org. Chem.* **1968**, *6*, 63. Bell, R. P. *Discuss. Faraday Soc.* **1965**, *39*, 16.

(4) Kurz, J. L.; Kurz, L. C. *J. Am. Chem. Soc.* **1972**, *94*, 4451.

(5) Marcus, R. A. *J. Phys. Chem.* **1968**, *72*, 891. Kreevoy, M. M.; Konasewich, D. E. *Adv. Chem. Phys.* **1971**, *21*, 243.

(6) Timoneda, J. J.; Hynes, J. T. *J. Phys. Chem.* **1991**, *95*, 10431.

(7) Aguilar, M. A.; Hidalgo, A. *J. Phys. Chem.* **1995**, *99*, 4293.

(8) Andrés, J. L.; Durán, M.; LLedós, A.; Bertrán, J. *Chem. Phys. Lett.* **1986**, *124*, 177.

(9) Whitnell, R. M.; Wilson, K. R. In *Reviews in Computational Chemistry*; Lipkowitz, K. B.; Boyd, D. B., Eds.; VCH Publishers: New York, 1993; pp 67−148.

(10) Muller, R. P.; Warshel, A. *J. Phys. Chem.* **1995**, *99*, 17516.

(11) Tuñón, I.; Martins-Costa, M. T. C.; Millot, C.; Ruiz-López, M. F. *J. Chem. Phys.* **1997**, *106*, 3633.

(12) Tuckerman, M.; Laasonen, K.; Sprik, M.; Parrinello, M. *J. Phys. Chem.* **1995**, *99*, 5749.

(13) Laasonen, K. A.; Klein, M. L. *J. Am. Chem. Soc.* **1994**, *116*, 11620. Laasonen, K. A.; Klein, M. L. *J. Phys. Chem.* **1997**, *101*, 98.

(14) Borgis, D.; Tarjus, G.; Azzouz, H. *J. Phys. Chem.* **1992**, *96*, 3188. Truong, T. N.; McCammon, J. A.; Kouri, D. J.; Hoffman, D. K. *J. Chem. Phys.* **1992**, *96*, 8136. Laria, D.; Ciccotti, G.; Ferrario, M.; Kapral, R. *J. Chem. Phys.* **1992**, *97*, 378. Borgis, D.; Tarjus, G.; Azzouz, H. *J. Chem. Phys.* **1992**, *97*, 1390. Borgis, D.; Hynes, J. T. *Chem. Phys.* **1993**, *170*, 315. Mavri, J.; Berendsen, H. J. C.; Van Gunsteren, W. F. *J. Phys. Chem.* **1993**, *97*, 13469. Mavri, J.; Berendsen, H. J. C. *J. Phys. Chem.* **1995**, *99*, 12717. Bala, P.; Grochowski, P.; Lesyng, B.; McCammon, J. A. *J. Phys. Chem.* **1996**, *100*, 2535. Lobaugh, J.; Voth, G. A. *J. Chem. Phys.* **1996**, *104*, 2056. Gelabert, R.; Moreno, M.; Lluch, J. M. *THEOCHEM* **1996**, *371*, 161. Tuckerman, M. E.; Marx, D.; Klein, M. L.; Parrinello, M. *Science* **1997**, *275*, 817. Vuilleumier, R.; Borgis, D. Submitted for publication.

(15) Ando, K.; Hynes, J. T. *J. Phys. Chem.* **1997**, *101*, 10464.

(16) Ruiz-López, M. F.; Rinaldi, D.; Bertrán, J. *J. Chem. Phys.* **1995**, *103*, 9249.

(17) Andrés, J. L.; Lledós, A.; Durán, M.; Bertrán, J. *Chem. Phys. Lett.* **1988**, *153*, 82.

(18) Tuñón, I.; Rinaldi, D.; Ruiz-López, M. F.; Rivail, J. L. *J. Phys. Chem.* **1995**, *99*, 3798.

(19) Xantheas, S. S. *J. Am. Chem. Soc.* **1995**, *117*, 10373.

(20) Grimm, A. R.; Bacskay, G. B.; Haymet, A. D. J. *Mol. Phys.* **1995**, *86*, 369.

(21) Novoa, J. J.; Mota, F.; Pérez del Valle, C.; Planas, M. *J. Phys. Chem. A* **1997**, *101*, 7842.

(22) Rivail, J. L.; Rinaldi, D. *Chem. Phys.* **1976**, *18*, 233. Rinaldi, D.; Ruiz-López, M. F.; Rivail, J. L. *J. Chem. Phys.* **1983**, *78*, 834. Rivail, J. L.; Rinaldi, D.; Ruiz-López, M. F. In *Theoretical and Computational Models for Organic Chemistry*; NATO ASI Series C, Vol. 339; Formosinho, S. J., Csizmadia, I. G., Arnaut, L., Eds.; Kluwer Academic Publishers: Dordrecht, The Netherlands, 1991; pp 79−92. Dillet, V.; Rinaldi, D.; Ángyán, J. G.; Rivail, J. L. *Chem. Phys. Lett.* **1993**, *202*, 18. Rivail, J. L.; Rinaldi, D. In *Computational Chemistry. Reviews of Current Trends, Vol. 1*; Leszczynski, J., Ed.; World Scientific: River Edge, NJ, 1996; pp 139−174.

(23) Ruiz-López, M. F.; Bohr, F.; Martins-Costa, M. T. C.; Rinaldi, D. *Chem. Phys. Lett.* **1994**, *221*, 109.

(24) Pierotti, R. A. *Chem. Rev.* **1976**, *76*, 717. Tuñón, I.; Silla, E.; Pascual-Ahuir, J. L. *Chem. Phys. Lett.* **1993**, *203*, 289.

(25) (a) Kim, H. J.; Hynes, J. T. *J. Am. Chem. Soc.* **1992**, *114*, 10508. (b) Kim, H. J.; Hynes, J. T. *J. Am. Chem. Soc.* **1992**, *114*, 10528. (c) Bianco, R.; Miertus, S.; Persico, M.; Tomasi, J. *Chem. Phys.* **1992**, *168*, 281. (d) Aguilar, M. A.; Olivares del Valle, F. J.; Tomasi, J. *J. Chem. Phys.* **1993**, *98*, 7375. (e) Basilevsky, M. V.; Chudinov, G. E.; Napolov, D. V. *J. Phys. Chem.* **1993**, *97*, 3270. (f) Mathis, J. R.; Bianco, R.; Hynes, J. T. *J. Mol. Liq.* **1994**, *61*, 81. (g) Tomasi, J. In *Structure and Reactivity in Aqueous Solution*; Cramer C. J., Truhlar, D. G., Eds.; ACS Symposium Series 568; American Chemical Society: Washington, DC, 1994; p 10.

(26) Hehre, W. J.; Ditchfield, R.; Pople, J. A. *J. Chem. Phys.* **1972**, *56*, 2257. Hariharan, P. C.; Pople, J. A. *Theor. Chim. Acta* **1973**, *28*, 213. Clark, T.; Chandrasekhar, J.; Spitznagel, G. W.; Schleyer, P. v. R. *J. Comput. Chem.* **1983**, *4*, 294.

(27) Frisch, M. J.; Trucks, G. W.; Schlegel, H. B.; Gill, P. M. W.; Johnson, B. G.; Wong, M. W.; Foresman, J. B.; Robb, M. A.; Head-Gordon, M.; Replogle, E. S.; Gomperts, R.; Andrés, J. L.; Raghavachari, K.; Binkley, J. S.; Gonzalez, C.; Martin, R. L.; Fox, D. J.; Defrees, D. J.; Baker, J.; Stewart, J. J. P.; Pople, J. A. *Gaussian 92/DFT*, Revision G.1; Gaussian, Inc.: Pittsburgh, PA, 1993.

(28) Pappalardo, R. R.; Rinaldi, D. *SCRFPAC*; QCPE No. 622; Indiana University: Bloomington, IN, 1992. D. Rinaldi, updated version of *SCRFPAC* (see ref 16).

(29) Tuñón, I.; Tortonda, F. R.; Pascual-Ahuir, J. L.; Silla, E. *THEOCHEM* **1996**, *371*, 117.

(30) Chirlian, L. E.; Francl, M. M. *J. Comput. Chem.* **1987**, *8*, 894. Breneman, C. M.; Wiberg, K. B. *J. Comput. Chem.* **1990**, *11*, 361.

(31) Strnad, M.; Martins-Costa, M. T. C.; Millot, C.; Tuñón, I.; Ruiz-López, M. F.; Rivail, J. L. *J. Chem. Phys.* **1997**, *106*, 3643.

(32) Warshel, A.; Werss, R. M. *J. Am. Chem. Soc.* **1980**, *102*, 6218.

(33) Warshel, A. *Proc. Natl. Acad. Sci. U.S.A.* **1978**, *75*, 5250. Warshel, A. *Proc. Natl. Acad. Sci. U.S.A.* **1984**, *81*, 444. Warshel, A.; Russel, S. T.; Churg, A. K. *Proc. Natl. Acad. Sci. U.S.A.* **1984**, *81*, 4785. Warshel, A.; Sussman, F.; Hwang, J. K. *J. Mol. Biol.* **1988**, *201*, 139.

(34) Luz, Z.; Meiboom, S. *J. Am. Chem. Soc.* **1964**, *84*, 4768. Loewenstein, A.; Szöke, J. *J. Am. Chem. Soc.* **1962**, *82*, 1151.

(35) Jorgensen, W. L.; Chandrashekar, J.; Madura, J. D.; Impeyand, R. W.; Klein, M. L. *J. Chem. Phys.* **1983**, *79*, 926.

(36) Note that the OO distance was also constrained in ref 11 although the value (2.9 Å) was a little longer than that used here (2.5 Å).

(37) Li, G.-S.; Maigret, B.; Ruiz-López, M. F. *J. Comput. Chem.* **1998**, *19*, 1675.

(38) (a) Lee, S.; Hynes, J. T. *J. Chem. Phys.* **1988**, *88*, 6853. (b) Lee, S.; Hynes, J. T. *J. Chem. Phys.* **1988**, *88*, 6863. (c) Truhlar, D. G.; Schenter, G. K.; Garrett, B. C. *J. Chem. Phys.* **1993**, *98*, 5756.

(39) Sitnitsky, A. E. *Chem. Phys. Lett.* **1995**, *240*, 47.